

Non-adiabatic quantum dynamics of the electronic quenching OH(A²Σ⁺)+Kr

Pablo Gamallo,^a Alexandre Zanchet,^b F. Javier Aoiz,^{*b} and Carlo Petrongolo^{*c}

^aDepartament de Ciència de Materials i Química Física & Institut de Química Teòrica i Computacional (IQTCUB), Universitat de Barcelona, c/ Martí i Franquès 1-11, 08028 Barcelona, Spain.

^bDepartamento de Química Física, Facultad de Química, Universidad Complutense, 28040 Madrid, Spain.

^cIstituto per i Processi Chimico Fisici, Consiglio Nazionale delle Ricerche, Via G. Moruzzi 1, 56124 Pisa, Italy.

*corresponding authors: aoiz@quim.ucm.es, carlopetrongolo41@gmail.com

Fig. 1S $r=1.916$ a.u. Π' PES/eV with respect to the reactants. Negative/zero/positive levels in red/black/blue. The Σ^+ - Π' diabatic crossing is labeled by a green line.

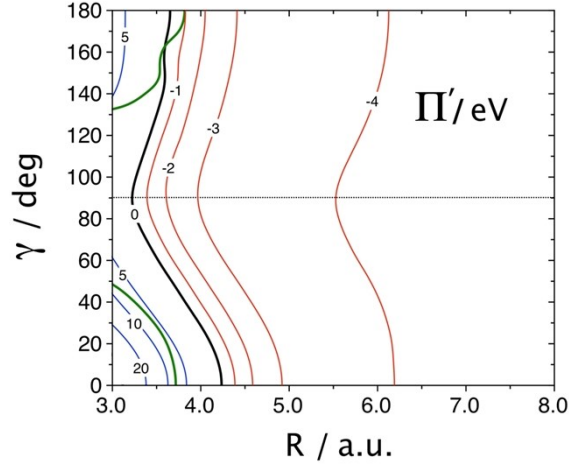
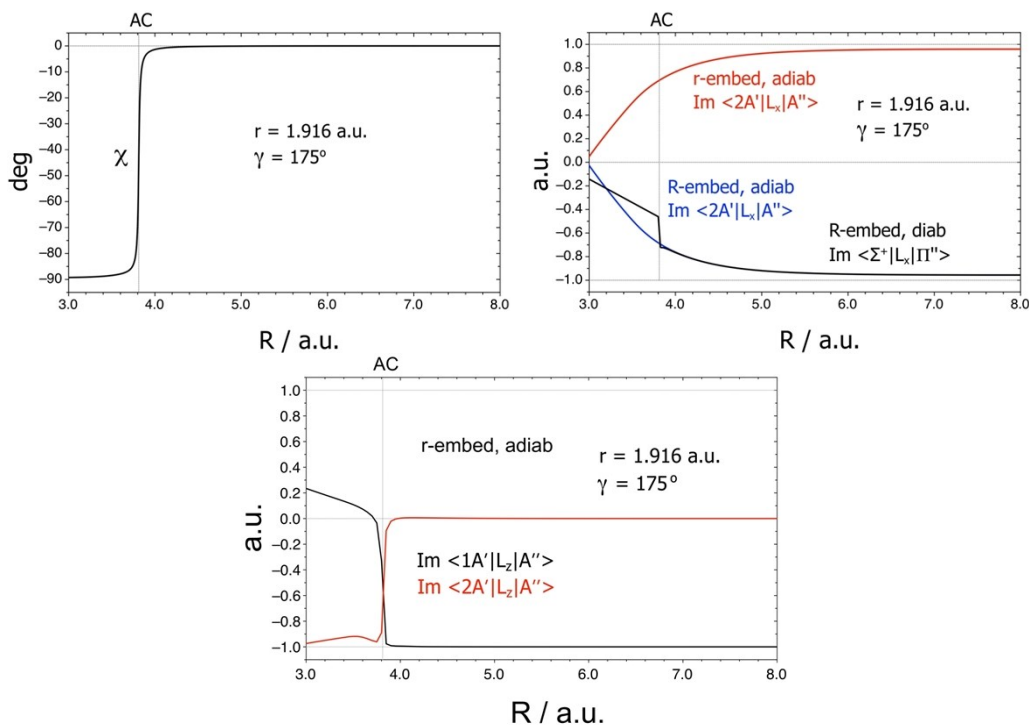


Fig. 2S $r=1.916$ a.u. and $\gamma=175^\circ$. Above: adiabatic-to-diabatic transformation angle χ and \hat{L}_x matrix elements in both embeddings and representations. Below: \hat{L}_z matrix element in the r -embedding and adiabatic representation. AC labels the avoided crossing $1A'-2A'$ at $R_{AC}=3.812$ a.u.



From Section 3 we have

$$\langle 2A' | \hat{L}_x | A'' \rangle = -\langle 2A' | \hat{L}_z | A'' \rangle \sin \gamma + \langle 2A' | \hat{L}_x | A'' \rangle \cos \gamma$$

$$\langle 1A' | \hat{L}_x | A'' \rangle = -\langle 1A' | \hat{L}_z | A'' \rangle \sin \gamma + \langle 1A' | \hat{L}_x | A'' \rangle \cos \gamma$$

$$\langle \Sigma^+ | \hat{L}_x | \Pi'' \rangle = \langle 1A' | \hat{L}_x | A'' \rangle \sin \chi + \langle 2A' | \hat{L}_x | A'' \rangle \cos \chi,$$

where \hat{L}_z and \hat{L}_x matrix elements are calculated with MOLPRO. The avoided crossing (AC) is at $R_{AC}=3.812$ a.u., $r=1.916$ a.u., and $\gamma=175^\circ$, very near to the conical intersection at 180° . Both χ and $Im \langle \Sigma^+ | \hat{L}_x | \Pi'' \rangle$ vary suddenly by traversing the avoided crossing and take their asymptotic values for OH($^2\Pi$)+Kr at large R , the former from -89 to 0° and the latter from -0.121 to -0.955 a.u. Note also that $Im \langle 2A' | \hat{L}_x | A'' \rangle \approx Im \langle \Sigma^+ | \hat{L}_x | \Pi'' \rangle$ at $R \geq R_{AC}$, where $2A' \approx \Sigma^+$ ($A''=\Pi''$ everywhere) and that all couplings fulfil the C_s and $C_{\infty v}$ selection rules.

Fig. 3S $r=1.916$ a.u. $\langle \Sigma^+ | \hat{L}_z^2 | \Pi' \rangle$, $\langle \Sigma^+ | \hat{L}_x \hat{L}_z | \Pi' \rangle$, and $Im \langle \Sigma^+ | \hat{L}_y | \Pi' \rangle$. Details as in Fig. 1S.

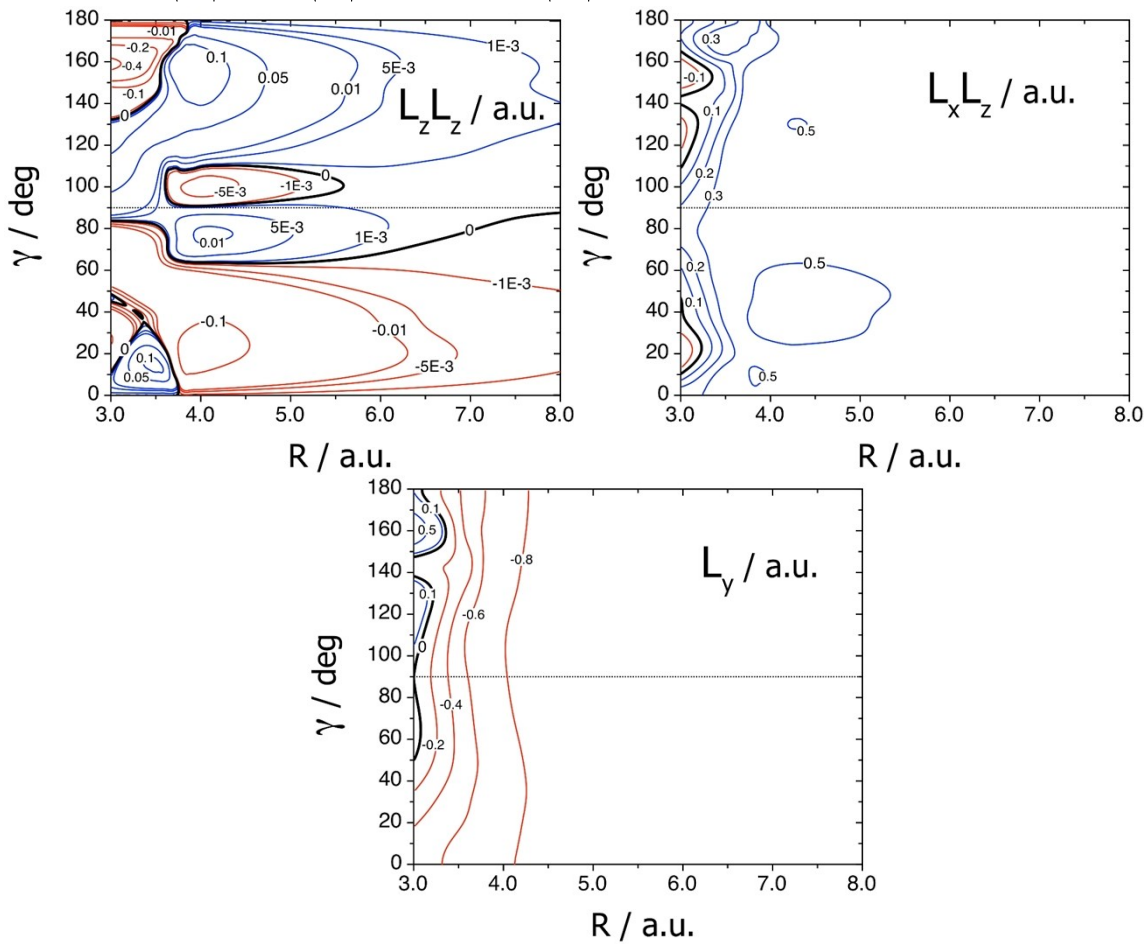


Fig. 4S $r=1.916$ a.u. $\text{Im} \langle \Sigma^+ | \hat{L}_z | \Pi'' \rangle$, $\text{Im} \langle \Sigma^+ | \hat{L}_x | \Pi'' \rangle$, $\text{Im} \langle \Pi' | \hat{L}_z | \Pi'' \rangle$, and $\text{Im} \langle \Pi' | \hat{L}_x | \Pi'' \rangle$. Details as in Fig. 1S.

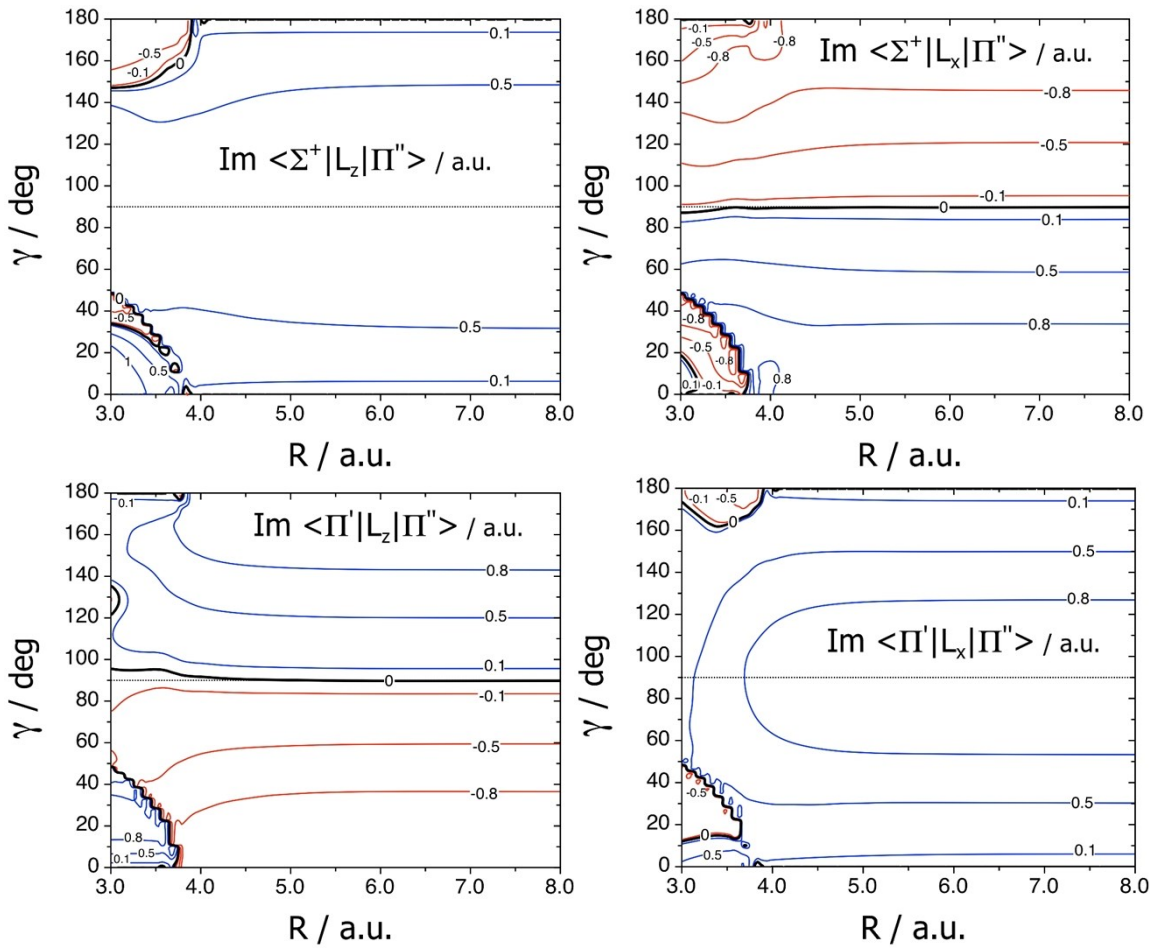


Fig. 5S $J=70$ and $j_0=K_0=0$. WP normalized norms and r -summed (R,γ) densities at 5 times.

